Published in final edited form as:
J Neurochem. 2010 July ; 114(1): 51–61. doi:10.1111/j.1471-4159.2010.06721.x.

Dopamine D_2 receptor function is compromised in the brain of the methionine sulfoxide reductase A knockout mouse

Derek B. Oien[*], **Andrea N. Ortiz**[†], **Alexander G. Rittel**[*], **Rick T. Dobrowsky**[*], **Michael A. Johnson**[†], **Beth Levant**[‡], **Stephen C. Fowler**[*], and **Jackob Moskovitz**[*]

[*] Department of Pharmacology and Toxicology, School of Pharmacy, University of Kansas, Lawrence, Kansas, USA

[†] Department of Chemistry, University of Kansas, Lawrence, Kansas, USA

[‡] Department of Pharmacology, Toxicology and Therapeutics, University of Kansas Medical Center, Kansas City, Kansas, USA

Abstract

Previous research suggests that brain oxidative stress and altered rodent locomotor behavior are linked. We observed bio-behavioral changes in methionine sulfoxide reductase A knockout mice associated with abnormal dopamine signaling. Compromised ability of these knockout mice to reduce methionine sulfoxide enhances accumulation of sulfoxides in proteins. We examined the dopamine D_2-receptor function and expression, which has an atypical arrangement and quantity of methionine residues. Indeed, protein expression levels of dopamine D_2-receptor were higher in knockout mice compared with wild-type. However, the binding of dopamine D_2-receptor agonist was compromised in the same fractions of knockout mice. Coupling efficiency of dopamine D_2-receptors to G-proteins was also significantly reduced in knockout mice, supporting the compromised agonist binding. Furthermore, pre-synaptic dopamine release in knockout striatal sections was less responsive than control sections to dopamine D_2-receptor ligands. Behaviorally, the locomotor activity of knockout mice was less responsive to the inhibitory effect of quinpirole than wild-type mice. Involvement of specific methionine residue oxidation in the dopamine D_2-receptor third intracellular loop is suggested by *in vitro* studies. We conclude that ablation of methionine sulfoxide reductase can affect dopamine signaling through altering dopamine D_2-receptor physiology and may be related to symptoms associated with neurological disorders and diseases.

Keywords

dopamine; dopamine receptor; locomotor activity; methionine oxidation; oxidative stress; post-translation modification

Post-translational modifications resulting from reactive oxygen species can alter the functions of many proteins. While most protein modifications by reactive oxygen species are irreversible,

Address correspondence and reprint requests to Dr. Jackob Moskovitz, Department of Pharmacology and Toxicology, University of Kansas, 1251 Wescoe Hall Drive, Malott 5064, Lawrence, KS 66045, USA. moskovij@ku.edu.

Supporting Information

Additional Supporting information may be found in the online version of this article:

Figure S1. Gαi/o protein expression levels in *MsrA*–/– and WT brains.

As a service to our authors and readers, this journal provides supporting information supplied by the authors. Such materials are peer-reviewed and may be re-organized for online delivery, but are not copy-edited or typeset. Technical support issues arising from supporting information (other than missing files) should be addressed to the authors.

methionine sulfoxide (MetO) modifications can be reversed by the methionine sulfoxide reductase (Msr) system, which consists of MsrA (reduces *S*-MetO) and MsrB (reduces *R*-MetO) (Moskovitz 2005). Reduction action of the Msr system may prevent irreversible protein damage, contribute to cellular antioxidant resistance, and regulate protein function. Evidence for a role of the Msr system in antioxidant defense is demonstrated by the adverse effects resulting from MsrA ablation (Moskovitz *et al.* 1995, 1997, 2001). Furthermore, over-expression of MsrA in various organisms and cells protects them from oxidative stress toxicity (Moskovitz *et al.* 1998; Ruan *et al.* 2002; Romero *et al.* 2004). The *MsrA* null mouse (*MsrA* −/−) is hypersensitive to oxidative stress, accumulates higher levels of carbonylated protein and expresses brain pathologies associated with neurodegenerative diseases (Moskovitz *et al.* 2001; Pal *et al.* 2007); this evidence suggests a major biological role of the Msr system. Furthermore, the Msr enzymes have been shown to switch several proteins between non-active and active forms by reducing specific MetO residues to methionine (Oien and Moskovitz 2008).

The *MsrA*−/− mouse exhibits age-dependent lower locomotor activity and abnormal gait indices (Oien *et al.* 2008) relative to control mice. Lower dopamine (DA) levels are associated with altered motor performance (Carlsson *et al.* 2007). Surprisingly, our recent observations showed that *MsrA*−/− brains in adult mice contained significantly higher levels of DA (Oien *et al.* 2008). Moreover, pre-synaptic neuronal DA in *MsrA*−/− striatal slices is released at higher DA pulses than wild-type (WT) slices as measured by fast scan cyclic voltammetry. These results raise the possibility that DA function is impaired in *MsrA*−/− mice. Moreover, *MsrA*−/− mice were less responsive to amphetamine treatment as assayed by locomotor activity and stereotypy, suggesting alteration of DA signaling. Dysfunctions of the corpus striatum and dopaminergic signaling are linked to a range of disorders including Parkinson's disease (Hornykiewicz 1962), Huntington's disease (Hickey *et al.* 2002), schizophrenia, and obsessive-compulsive disorder (Saxena *et al.* 1998).

The observed *MsrA*−/− locomotor deficits and DA abnormalities prompted us to further examine DA signaling events that are associated with striatal movement pathways. The dopamine D_1 receptor (D1DR) and dopamine D_2 receptor (D2DR) are closely associated with movement regulation, and theoretically are the DA receptors most related to the *MsrA*−/− locomotor phenotypes (Oien *et al.* 2008). In addition, D2DR is also expressed in its short form ($D2DR_S$) that serves as an autoreceptor for dopaminergic neurons. Thus, methionine oxidation in either the long form of D2DR or $D2DR_S$ or a combination of both may be related to the elevation in DA levels observed in *MsrA*−/− brains (Oien *et al.* 2008). In the current study we investigate the ligand-binding capabilities of DA receptors and their coupling efficiency to G-proteins in *MsrA*−/− versus WT mice. The presented data support the hypothesis that MetO modification to D2DRs participates in the *MsrA*−/− behavioral and biochemical phenotypes.

Materials and methods

Materials

The radioligands [^{3}H]SCH23390 (85 Ci/mmol), [^{3}H]raclopride (84 Ci/mmol), [^{3}H]quinpirole (50 Ci/mmol), were purchased from Perkin Elmer (Waltham, MA, USA). Non-radioactive sulpiride, quinpirole, SKF82958, and GTPγS were purchased from Sigma, St Louis, MO, USA. Mouse and goat antibodies against D2DR were purchased from Abcam (Cambridge, MA, USA). Mouse β-actin antibodies were purchased from Molecular Probes, Eugene, OR, USA.

Mice

Mice used in these studies were WT (C57BL6/129 Sv) and *MsrA*−/− on the same genetic background at an age of 6–8 months unless otherwise noted. Both types of mice were littermates

born to *MsrA*+/− heterozygous parents (Moskovitz *et al.* 2001). All procedures using mice were performed within guidelines of the NIH and KU Institutional Animal Care and Use Committee.

Immunohistochemistry analysis

Coronal brain sections from 12-month-old WT and *MsrA*−/− mice were processed as 20 μm-thick brain sections. Sections were treated with 3% H_2O_2 in methanol for 30 min. After blocking with 1% bovine serum albumin and 3% horse serum in phosphate-buffered saline, the sections were incubated for 24 h with primary goat antibodies against D2DR (1 : 500 dilution, stock concentration of 1.5 mg/mL). Sections were then incubated with biotinylated mouse anti-goat IgG antibodies (Santa Cruz Biotechnology, Santa Cruz, CA, USA), avidin–horseradish peroxide solution, 0.015% diaminobenzidine, 0.001% H_2O_2, and finally counter-stained with hematoxylin. The brain slides were washed, dehydrated, mounted, and visualized using a brightfield microscope with a 100× objective lens.

Immunoblot analysis

Equal amounts of striatal membranal protein extracts or cytosolic brain proteins (extracted as described below for receptors fraction) were subjected to sodium dodecyl sulfate-gel electrophoresis. Immunoblot analyses with anti-goat D2DR antibodies (1 : 1000 dilution, stock concentration of 1.5 mg/mL) were performed according to common procedures. β-actin (loading control) was detected by primary anti-β-actin mouse antibodies.

Antagonists and agonists binding of D1DR and D2DR ligands

Saturation curves of receptor binding were determined by using the common membrane filtration assay (Bylund and Toews 1993). Briefly, brains (striatal region of each mouse type) were dissected and glass-Teflon homogenized in phosphate-buffered saline with protease inhibitor cocktail (Roche Molecular Biochemicals, Indianapolis, IN, USA). Following centrifugal precipitation at 20 000 *g* for 20 min, the supernatant was removed and saved (cytosolic fraction in immunoblots), and the membranal pellet was washed and precipitated again by centrifugation. Final pellet was homogenized in 1.0 mL of 50 mM Tris pH 7.4. Membranal protein fractions of 100 μg were used per assay, determined by BCA Protein Assay Kit (Thermo Scientific, Waltham, MA, USA). Total ligand binding was determined following incubation of membranal fractions with incrementing concentrations of radioligand for 2 h at 25°C. Non-specific ligand binding was determined using the same conditions with the addition of non-radioactive ligands, 1 mM DA for D1DR and 1 μM sulpiride for D2DR. Bound radioligand was separated using a Brandel harvester (Brandel, Gaithersburg, MD, USA). Radioligand bound to the filter was measured by liquid scintillation counting. Specific ligand binding values were calculated by subtracting non-specific ligand binding from total ligand binding. The ligands used in the tests were: [^{3}H]SCH23390 and [^{3}H]raclopride as D1DR and D2DR antagonists, respectively, and [^{3}H]quinpirole as a D2DR agonist. The range for radioactive materials used was between 0.03 nM and 4.0 nM (increments by serial dilution).

The effect of MsrA enzyme on quinpirole and raclopride binding was tested by using recombinant yeast MsrA (10 μg) (Moskovitz *et al.* 1997) with 15 mM dithiothreitol (DTT; this alone did not affect binding). D1DR binding to the agonist SKF82958 was determined using the same conditions above, except for the addition of 2 nM [^{3}H]SCH23390 to quantify the competitive binding of non-radiolabeled SKF82958 ligand (performed because of limited sources of commercially available radiolabeled D1DR agonists).

GTPγS-induced inhibition of radiolabeled quinpirole binding to D2DR

The ability of agonists to stimulate the dissociation of GDP and association of GTP from G-protein was assessed using GTPγS, a non-hydrolyzable analogue of GTP (Zhang *et al.* 2001). When the agonist binds to the receptor, GDP is released from the G-protein and GTPγS binds (Harrison and Traynor 2003). The G-protein uncoupling on [^{3}H]quinpirole binding to the D2DR was investigated by measuring the inhibition of [^{3}H]quinpirole binding at incrementing GTPγS concentrations. The membrane portion of homogenized striatal regions were isolated and lysed in 5 mM Tris buffer by glass-Teflon homogenation. Membranal extracts (30 mg/mL; 80 μg per assay) were incubated with [^{3}H]quinpirole (1 nM) and GTPγS (0.1, 1, 10, 100, and 1000 nM) in 50 mM Tris buffer for 2 h at 25°C in a total volume of 1 mL. To determine non-specific binding, identical assays were performed in the presence of sulpiride (1 μM; racemic mixture). Unbound ligand was removed by Brandel filtration and the remaining bound ligand was quantified by liquid scintillation counting.

Stimulated release of DA in striatal brain sections in the presence of quinpirole and sulpiride measured by fast scan cyclic voltammetry

Brain sections were prepared as previously described (Johnson *et al.* 2006). Mice were anesthetized by isoflurane inhalation. The brain was immediately removed and placed in ice cold artificial CSF. Artificial CSF consisted of 126 mM NaCl, 2.5 mM KCl, 1.2 mM NaH_2PO_4, 2.4 mM $CaCl_2$, 1.2 mM $MgCl_2$, 25 mM $NaHCO_3$, 20 mM HEPES, and 11 mM D-Glucose at pH 7.4 and was continuously saturated with 95% O_2/5% CO_2 throughout the experiment. Coronal sections of 300 μm in thickness were made using a vibratome slicer (Leica Microsystems, Bannockburn, IL, USA). A single section was placed in the superfusion chamber with artificial CSF flowing at 34°C and a continuous rate of 2 mL/min. Each brain section was equilibrated for 60 min prior to obtaining measurements. Quinpirole and sulpiride in artificial CSF were maintained in a separate reservoir and introduced through a three-way valve.

Carbon-fiber microelectrodes were fabricated as previously described (Kraft *et al.* 2009). A single carbon-fiber with a 7 μm diameter (Goodfellow Cambridge Ltd., Oakdale, PA, USA) was aspirated through a glass capillary tube (1.2 mm outer diameter, 0.68 mm inner diameter, 4 inches long, A-M Systems, Inc., Sequim, WA, USA) and pulled using a heated coil puller (Narishige International USA, Inc., East Meadow, NY, USA). Electrodes were trimmed to 20 μm from the glass seal, further insulated with epoxy resin (EPON resin 815C, EPIKURE 3234 curing agent, Miller-Stephenson, Morton Grove, IL, USA), and then cured at 100°C for 1 h. Prior to experimentation, electrodes were backfilled with 0.5 M potassium acetate.

A triangular waveform starting at −0.4 V, increasing to +1.0 V, and scanning back to −0.4 V was applied at the carbon-fiber working electrode. A scan rate of 300 V/s was used with an update rate of 10 Hz. A head-stage amplifier (UNC Chemistry Department Electronics Design) was interfaced with a computer via breakout box and custom software provided by R.M. Wightman and M.L.A.V. Heien. A choridated silver wire was used as an Ag/AgCl reference electrode. The carbon fiber was inserted 100 μm into the dorsolateral caudate-putamen region of the striatum. The fiber was between the prongs of a bipolar stimulation electrode (Plastics One, Roanoke, VA, USA), which were separated by 200 μm. Current was measured at 0.6 V, which is the oxidation potential for DA. DA release was measured in the presence of either 1 μM quinpirole or 5 μM sulpiride as previously described (Fawaz *et al.* 2009) using a 30-pulse stimulus train at a stimulation frequency of 60 Hz. During stimulation and DA release, stabilized scans of 15 s were collected every 2 min and averaged as 4-min time blocks.

Locomotor activity measured by force-plate actometer

The force-plate actometer and methods of data analysis have been previously described (Fowler *et al.* 2001). Briefly, the force-plate actometer consists of a low mass and highly stiff 5 mm thick plate (28 cm × 28 cm). This plate is supported by four Sensotec Model 31 load cells (0–250 g range). Each force plate is positioned below a Plexiglas cage that confines the mouse to the force-sensing plate and is encased in sound-attenuating cubicle. Horizontal movements of the mouse were recorded along the sensing surface with a spatial resolution of 1 mm and a temporal resolution of 0.01 s.

The duration of recording sessions was based upon preliminary experiments and relevant literature assessing spontaneous locomotor activity (Geter-Douglass *et al.* 1997; Usiello *et al.* 2000; Wang *et al.* 2000). The effects of the drugs used on locomotor activity were apparent within the initial period of 45 min following drug injection. Thus, 45-min periods were determined to be sufficient to monitor the locomotor response to the performed treatments. Total distance traveled per animal was measured and analyzed by 2-way ANOVA (two mouse types) with repeated measures on the time block and session factors.

Administration of agonists of D1DR and D2DR for locomotor activity analyses

Prior to treating the mice with D1DR or D2DR agonists, the WT and *MsrA*−/− mice received intraperitoneal injection with 0.9% saline as a vehicle control and spontaneous locomotor activity was monitored for 45 min using force-plate actometers. After 4 days, the same mice were injected with either quinpirole (D2DR agonist, 0.1 and 0.5 mg/kg) or SKF82958 (D1DR agonist, 0.3 and 1.0 mg/kg) and locomotor activity was monitored for 45 min. A minimum of 4 days between trials was used to minimize potential carryover effects. Different sets of animals were used for each drug to prevent cross-reactivity and carryover effects between drugs. The drugs were administered at volume of 5 mL/kg.

MetO residues in recombinant long form of D2DR third intracellular loop

The long form of rat D2DR third intracellular loop ($D2DR_L$-IC_3) was expressed as a glutathione S-transferase (GST) fusion protein in bacteria (gift from Dr. Kim Neve, Oregon Health & Science University) and purified according to published procedures (Lan *et al.* 2009). The protein was oxidized overnight with 200 mM H_2O_2 and excess oxidants were removed by catalase. In parallel, oxidized protein was reduced with recombinant poly-His-tagged yeast MsrA (10 μg) (Moskovitz *et al.* 1997) in the presence of 20 mM DTT for 1 h at 37°C (DTT alone does not reduce MetO residues under these conditions). After reduction, all proteins (non-treated, H_2O_2-treated, and MsrA-reduced) were subjected to gel-electrophoresis followed by Commassie blue staining for the isolation of the corresponding GST-$D2DR_L$-IC_3. Bands corresponding to the predicted weight of ~54 kDa were excised and protein was isolated. The protein was subjected to tryptic digestion prior to analysis by a LCT Premier electrospray ionization tandem mass spectrometer (Waters Corp., Milford, MA, USA). The mass spectrometry analyses of the peptides and their MetO content were performed according to previously published methods (Zhang *et al.* 2010).

Results

Expression levels and ligand binding capabilities of D2DR in MsrA−/− striatum

Postmortem brain sections from *MsrA*−/− and WT mice were immunostained with anti-D2DR antibodies. The *MsrA*−/− striatal region exhibited higher reaction levels with the antibodies compared with this region in WT mice (Fig. 1a). D2DR expression levels were quantified by immunoblot analysis on brain extracts followed by densitometry analysis (Fig. 1b). Similar to

the increase of DA in *MsrA*−/− brains (Oien *et al.* 2008), the up-regulation of the D2DR may be part of compensatory response for the dysfunction of the DA system in the *MsrA*−/− brain.

The binding of the D2DR to appropriate ligands can reflect their expression levels and function in signaling. Binding of the D2DR antagonists are independent of G-protein coupling and more reflective of D2DR expression levels. Binding of the D2DR agonists are dependent on G-protein coupling and more reflective of D2DR function in signaling. Accordingly, the calculated B_{max} value of D2DR antagonist [^{3}H]raclopride was higher in *MsrA*−/− membranal fractions (250 ± 20 fmole/mg protein) compared with the value of WT (140 ± 4 fmole/mg protein) (Fig. 2a). In addition, the K_d value for [^{3}H]raclopride in both mouse types was similar (K_d of 0.70 ± 0.10 nM), suggesting no difference in the binding affinity of the bound antagonists to D2DR (it is noteworthy that the K_d values in these mice are different than rats, see 'Discussion'). The [^{3}H]raclopride B_{max} values also provide further supportive evidence to the observed elevated levels of the D2DR in *MsrA*−/− brain (Fig. 1). The calculated B_{max} value of D2DR agonist [^{3}H]quinpirole was lower in *MsrA*−/− membranal fractions (56 ± 7 fmole/mg protein) when compared with the value of the WT (140 ± 10 fmole/mg protein), while the K_d value for [^{3}H]quinpirole binding was similar in both mouse types (0.40 ± 0.05 nM) (Fig. 2a). These observations suggest that the coupling ability of the *MsrA*−/− D2DR to the respective G-proteins is compromised, in spite of the higher number of receptors in *MsrA*−/− mice (Fig. 1). In addition, adding recombinant MsrA to the binding reaction mixture caused significant recovery of the *MsrA*−/− [^{3}H]quinpirole B_{max} value to the WT B_{max} value (Fig. 2b). This latter result strengthens the hypothesis that lack of MsrA enhances MetO formation in D2DR, which affects D2DR function and expression. In contrast to relative D2DR agonist-to-antagonist B_{max} differences between the two mouse types (Fig. 2a and b), no significant differences were found for D1DR ligand binding to the antagonist SCH23390 or agonist SKF82958 between these mouse types (Fig. 2c and d). At relatively high concentrations, [^{3}H]SCH23390 was bound to *MsrA*−/− and WT striatal fractions to a similar extent (Fig. 2c). Similar results were found when SKF82958 was used (Fig. 2d). The SKF82958 ligand was not radiolabeled, thus binding efficiency was determined by its competitive binding in the presence of 2 nM [^{3}H]SCH23390 as previously described (Nwaneshiudu and Unterwald 2009). The amounts of [^{3}H]SCH23390 bound to the striatal fractions were significantly decreased ($p < 0.05$) by the presence of 16 nM of SKF82958. This supports the hypothesis that *MsrA* ablation primarily impacts the D2DR.

G-protein coupling efficiency to D2DR in MsrA−/− striatum

The non-hydrolyzable GTPγS analog will reduce the binding of [^{3}H]quinpirole to D2DR (quinpirole binds with lower affinity to uncoupled D2DR compared with coupled receptors). Consequently, competition curves were performed by inhibiting [^{3}H]quinpirole binding with increasing concentrations of GTPγS. Accordingly, the maximal inhibition from the competition curve reflects the number of D2DR coupled to G-proteins, while the 50% binding inhibition concentration (IC_{50}) from the curve reflects the potency of GTPγS to dissociate the D2DR and G-protein complex. The maximum binding of [^{3}H]quinpirole to D2DR in *MsrA*−/− was ~50% of the maximum binding of the agonist to the receptors in the WT brain (Fig. 3; WT = 50 ± 6 and *MsrA*−/− = 26 ± 3 fmole/mg protein in the presence of 1 μM [^{3}H]quinpirole). The IC_{50} was found to be similar for both mouse types (10 ± 1 nM), which is in agreement with current literature (Zhang *et al.* 2001). These data suggest reduced G-protein and D2DR coupling in the *MsrA*−/− brain. Moreover, the similar IC_{50} in both mouse types suggests that the dissociation rates of the receptors from the G-proteins are similar. The reduced interaction of G-proteins with D2DR in *MsrA*−/− brains could be a consequence of either lower G-protein expression or interference in the initial binding of G-proteins to the third intracellular loop of D2DR. There was no significant difference in expression of $G\alpha_{i/o}$ proteins between the two mouse types (Figure S1), suggesting that the observed limitation in *MsrA*−/− D2DR agonist

binding is probably not because of reduced $G\alpha_{i/o}$ levels. Since the expression levels of these G-proteins seem to be similar in the two mouse types (Figure S1), data in Fig. 3 are supportive of compromised D2DR agonist binding in *MsrA*−/− brains (Fig. 2a) and also may reflect interference in binding of *MsrA*−/− G-proteins to the third intracellular loop of D2DR.

Pre-synaptic stimulated dopamine release of MsrA−/− striatal tissue sections in response to D2DR ligands

A shorter form of the D2DR, $D2DR_S$, serves as an autoreceptor on the pre-synaptic membrane of dopaminergic neurons. This receptor has a third intracellular loop that is truncated by 29 amino acids, but still retains four of the eight methionine residues. $D2DR_S$ has been previously demonstrated to respond to the D2DR agonist quinpirole and D2DR antagonist sulpiride by decreasing and increasing the pre-synaptic release of DA, respectively (Fawaz *et al.* 2009). Using a similar experimental design as Fawaz *et al.*, the pre-synaptic DA release in the striatal area from *MsrA*−/− and WT coronal sections was measured in the presence of quinpirole (Fig. 4a and b) and sulpiride (Fig. 4c and d). Pre-synaptic DA release was detected by fast scan cyclic voltammetry every 2 min, initially without any treatment and followed by treatment with a saturating dose of quinpirole. In the presence of quinpirole, *MsrA*−/− sections were less responsive than WT sections when both were compared to the respective initial stimulation and detection without the presence of drug. The DA release of the *MsrA*−/− pre-synaptic neurons was significantly higher than the decreased release of the WT pre-synaptic neurons ($p < 0.05$; two-way repeated measures ANOVA). Moreover, the *MsrA*−/− pre-synaptic neurons were also less responsive to sulpiride than WT. After sulpiride treatment, the changes in DA concentration from the initial non-treated measurement of *MsrA*−/− slices were significantly lower than the increased DA concentration changes of the WT ($p < 0.05$). These results suggest that the $D2DR_S$ signaling is disrupted in *MsrA*−/− mice.

Locomotor activity of MsrA−/− mice after injections of dopamine receptor agonists

The *in vitro* and brain section findings suggest functional changes in the DA system that should be expressed at the behavioral level. Consequently, we investigated the behavioral effects of D1DR and D2DR selective agonists on locomotor activity in *MsrA*−/− and WT mice. A significant difference in locomotor activity was observed between the mouse strains when injected with quinpirole. At a dose of 0.5 mg/kg, the *MsrA*−/− exhibited ~40% more locomotor activity than WT, and at a dose of 0.1 mg/kg the *MsrA*−/− exhibited ~35% more locomotor activity than WT (Fig. 5a; repeated measures ANOVA for mouse type effect, $p < 0.02$). No significant difference in locomotor activity was observed between the two mouse types when injected with saline (Fig. 5), which is consistent with previous experiments (Oien *et al.* 2008). Given the higher expression level of the D2DR in *MsrA*−/− mice, these data suggest that the compromised responsiveness of the *MsrA*−/− D2DRs to the inhibitory effect of quinpirole may be because of irregularities in either DA binding or abnormal function of further downstream signaling events. Moreover, the lack of a significant dose effect in the quinpirole concentrations used is consistent with published data, illustrating by similar analyses that there was no dose effect in mice even at broader and higher dose ranges (Wang *et al.* 2000).

In addition, *MsrA*−/− and WT mice were injected with two doses of the D1DR agonist SKF82958, and ensuing locomotor activity behavioral effects were assessed in 45-min sessions (Fig. 5b). The ANOVA applied to these distance traveled data indicated no effect of mouse type, a significant effect of SKF82958 dose effect (repeated measures ANOVA; $p < 0.01$), and no dose-by-type interaction. These data show that the D1DR agonist did not differentially affect the two types of mice (no type effect, no interaction effect). As expected from the literature for several types of inbred mice, SKF82958 substantially increased locomotor activity in the dose range used here (Niimi *et al.* 2009). These data strengthen the idea that methionine oxidation in the D2DR third cytoplasmic loop plays an important role in the *MsrA*−/−

phenotype (the D2DR third intracellular loop contains eight methionines, and the D1DR C-terminus cytoplasmic region contains only one methionine; both of these regions are directly involved in signal transduction).

MetO residues in recombinant long form D2DR third intracellular loop

Oxidation vulnerability was examined with recombinant GST-D2DR$_L$-IC$_3$ and peroxide exposure. Non-H_2O_2 oxidized GST-D2DR$_L$-IC$_3$ protein, H_2O_2 oxidized GST-D2DR$_L$-IC$_3$ protein, and H_2O_2 oxidized GST-D2DR$_L$-IC$_3$ proteins treated with MsrA were all subjected to mass spectrometry analysis following gel-electrophoresis separation and tryptic digestion. The procedure used to detect peptides by this mass spectrometry analysis (Zhang *et al.* 2010) normally causes some methionine oxidation. To compensate for this, averaged MetO levels detected in the non-H_2O_2 oxidized GST-D2DR$_L$-IC$_3$ peptides were subtracted from the H_2O_2 oxidized forms of the protein (+/− MsrA and DTT). A 17-amino-acid peptide produced by collision-induced dissociation was found to contain the highest quantity of oxidized methionine (276-AQELEMEMLSSTSPPER-292; Fig. 6). Furthermore, the Met283 residue (present in daughter ion Y10) of the peptide was found to be relatively more oxidized in comparison with the Met281 residue (present in daughter ion Y12; data not shown). The net oxidation level of Met283 treated with H_2O_2 *in vitro* was on average 2% (Fig. 6). This oxidation level resembles the basal physiological level of MetO in unpublished observations and in yeast cells without H_2O_2 in the growth media (Moskovitz *et al.* 1997). Accordingly, the current *in vitro* condition of oxidation may resemble physiological methionine oxidation. The addition of MsrA and DTT to oxidized GST-D2DR$_L$-IC$_3$ protein was able to reduce the sulfoxide of Met283 by 60% (Fig. 6). The MsrA enzyme can reduce only the *S*-form of MetO. Empirically, the distribution ratio of *S* to *R* forms of MetO is 1 : 1 (Oien and Moskovitz 2008). Typically, we observed that *in vitro* oxidation of methionine by H_2O_2 results in 60% *S*-MetO and 40% *R*-MetO (determined by amino acid analysis separation; unpublished results). Thus, the ability of the MsrA to reduce 60% of the total oxidized Met283 reflects the expected maximum reduction capability of the enzyme in an expected MetO racemic mixture of *R* and *S* forms following methionine oxidation by H_2O_2. In addition, the preferred oxidation of Met283 suggests this residue is more vulnerable to oxidation and also readily accessible to the reducing function of MsrA.

Discussion

This study describes for the first time the possible effects of methionine oxidation on DA receptor function *in vivo* by using *MsrA*−/− mice. Previously, we observed an inverse relationship between abnormally high levels of DA accompanied by lowered locomotor activity in *MsrA*−/− mice (Oien *et al.* 2008). This is paradoxical because chronically low levels of brain DA are associated with Parkinson's disease-like motor effects including low levels of locomotor activity. These unexpected results led us to investigate that the alteration of DA receptor function and expression may be involved.

Both the D1DR and the D2DR modulate striatal information processing that is integral to the translation of cortical plans into actions by providing for the expression of selected motor responses with concurrent suppression of unwanted responses ('responses' may be cognitive or motor). The D2DR are of particular clinical interest because of their role in neuropsychiatric disorders, such as schizophrenia, where D2DR antagonists are therapeutic (Lieberman *et al.* 2008), or their role in the movement disorder, Parkinson's disease, where D2DR agonists are known to benefit patients (Pahwa *et al.* 2004). Thus, we predicted a reduced expression of striatal D2DR in *MsrA*−/− mice to explain the relative lower locomotor activity (Oien *et al.* 2008). Surprisingly, there was an increase of D2DR expression in *MsrA*−/− mice (Fig. 1). Higher levels of [^{3}H]raclopride binding to D2DR confirmed this increase (Fig. 2). The higher

protein levels of the D2DR in *MsrA*−/− may be part of a compensatory mechanism for the accumulation of oxidized D2DR. In spite of the higher D2DR levels observed, the binding of [^{3}H]quinpirole suggests a compromised agonist binding of the D2DR in *MsrA*−/− brain (Fig. 2a). Supportive *in vivo* data to this phenomenon are demonstrated by the lesser D2DR agonist inhibitory effect on locomotor function in *MsrA*−/− mice (Fig. 5a). Agonist occupation of G-protein coupled receptors leads to a cellular response that wanes, or desensitizes, with prolonged agonist exposure. MetO in the intracellular loops of the D2DR may cause a conformational change that may result in uncoupling of the receptor to G-protein subunits. The relative compromised binding of the D2DR to [^{3}H]quinpirole suggests lower efficiency in D2DR-G-protein coupling. Indeed, our data show that although the levels of $G\alpha_{i/o}$ are similar in both mouse types (Figure S1), the coupling of D2DR to G-proteins is reduced by ~50% in *MsrA*−/− relative to WT brain (Fig. 3). This suggests that the total $G\alpha_{i/o}$ coupling capacity is reduced in *MsrA*−/− brain rather than their coupling affinity to D2DR.

The ability of MsrA to restore D2DR agonist binding in *MsrA*−/− striatal extracts (Fig. 2b) supports the theory that methionine oxidation of D2DR occurs in the *MsrA*−/− brain. Accordingly, it may be beneficial to cause striatal over-expression of Msr to prevent MetO related abnormalities manifested by oxidized D2DR. Furthermore, the selectivity of the effect of methionine oxidation on D2DR (by MsrA ablation) was demonstrated by the similar binding of D1DR to striatal extracts in both mouse types (Fig. 2c and d). Data presented in Fig. 4 suggest the autoreceptor function of D2DR in *MsrA*−/− striatum is compromised in its functional response to quinpirole and sulpiride compared to WT $D2DR_S$. The *in vivo* observation that *MsrA*−/− mice are less responsive to the inhibitory effect of quinpirole on locomotor activity (Fig. 5a) supports the conclusion that there is a general malfunction of *MsrA*−/− D2DR. Furthermore, the *in vivo* specificity of the MsrA ablation effect to D2DR is strengthened by the similar response of both mouse types to D1DR agonist (Fig. 5b). According to the literature, the use of the administrated doses of 0.1 and 0.5 mg/kg quinpirole are within the common range used in mice. In mice, there is no increased locomotor response as the dose is increased; instead, a suppression of locomotor activity is observed (Geter-Douglass *et al.* 1997;Usiello *et al.* 2000;Wang *et al.* 2000). Mice are different from rats in their response to quinpirole. In rats there is an increase of locomotor response with a higher quinpirole dose (Eilam *et al.* 1991;Koeltzow *et al.* 2003). This observation maybe is linked to observed difference in the ligand K_d values in rats (Levant *et al.* 1992) vs. mice (current study).

Taken together, it is suggested that lack of MsrA leads to methionine oxidation in both long and short forms of D2DR and diminishes their overall function efficacy. The general lowered *MsrA*−/− response to quinpirole, both *in vitro* and *in vivo* (Figs 2 and 5) implies that conserved regions of both D2DR subtypes are primarily affected in the *MsrA*−/− mouse (this does not exclude involvement of the 29 amino acid sequence that is not present in the $D2DR_S$). The compromised G-protein coupling in *MsrA*−/− may be a result of oxidative modification of specific methionine residues, especially in the cytoplasmic loops of the D2DR that are important for G-proteins coupling (i.e. $D2DR_L$-IC_3) (Montmayeur *et al.* 1993;Ilani *et al.* 2002). To assess the possibility of methionine oxidation in $D2DR_L$-IC_3 and reversal by MsrA *in vitro*, a recombinant GST-$D2DR_L$-IC_3 protein was oxidized and treated with recombinant MsrA. An oxidation of a specific methionine (Met283) in recombinant GST-$D2DR_L$-IC_3 protein occurred and was reduced to methionine by 60% with MsrA (Fig. 6). Met283 is present in both subtypes of D2DR and may be an important target for oxidation that affects the general function of this receptor. Future experiments are underway to monitor *in vivo* MetO levels and location in the D2DR of *MsrA*−/− mice. Overall, the collective evidence indicates that primarily D2DR related signaling is affected in *MsrA*−/− mice. However, the contributions of other signaling events to the observed abnormalities will still need further investigations.

Mechanistically, we suggest that oxidation of specific methionine residues may also affect phosphorylation of adjacent amino acids in $D2DR_L$-IC_3, thereby altering DA signal transduction pathways. For example, a regulatory role of MetO in protein phosphorylation was recently reported (Emes 2009; Hardin *et al.* 2009; Oien *et al.* 2009). Accordingly, it is possible that specific MetO residues in $D2DR_L$-IC_3 inhibit phosphorylation events that are important for proper coupling of the receptor to G-proteins as well (Namkung *et al.* 2009).

Our data can be interpreted to suggest that lack of MsrA in mouse brain causes D2DR malfunction via G-protein uncoupling leading to the production of higher DA levels (as a potential compensatory mechanism), reduced locomotor activity, and diminished behavioral responsiveness to D2DR agonists (Oien *et al.* 2008). Understanding the role of MsrA and MetO in DA physiology may result in identifying other proteins and neurotransmitter receptors that are altered by oxidative modification of methionine.

Recently, it was reported that mutations in the upstream region of *MsrA* may be potential markers for schizophrenia. If this proves true, research clearly supports the relevance of the *MsrA*−/− DA system to the occurrence of DA-related abnormal behavior (Walss-Bass *et al.* 2009).

Supplementary Material

Refer to Web version on PubMed Central for supplementary material.

Acknowledgments

This study was supported by the KIDDRC Center (HD02528), National Institutes of Health (AG027363, NS054847, DK073594), and the KU School of Pharmacy (General Research Fund). We thank Jade M. Franklin for her technical assistance.

Abbreviations used

D1DR	dopamine D_1 receptor
D2DR	dopamine D_2 receptor
$D2DR_L$-IC_3	third intracellular loop of dopamine D_2 receptor
$D2DR_S$	short form dopamine D_2 receptor
DA	dopamine
DTT	dithiothreitol
GST	glutathione S-transferase
MetO	methionine sulfoxide
Msr	methionine sulfoxide reductase
WT	wild-type

References

Bylund DB, Toews ML. Radioligand binding methods: practical guide and tips. Am J Physiol 1993;265:L421–L429. [PubMed: 8238529]

Carlsson T, Bjorklund T, Kirik D. Restoration of the striatal dopamine synthesis for Parkinson's disease: viral vector-mediated enzyme replacement strategy. Curr Gene Ther 2007;7:109–120. [PubMed: 17430130]

Eilam D, Clements KV, Szechtman H. Differential effects of D1 and D2 dopamine agonists on stereotyped locomotion in rats. Behav Brain Res 1991;45:117–124. [PubMed: 1686397]

Emes MJ. Oxidation of methionine residues: the missing link between stress and signalling responses in plants. Biochem J 2009;422:e1–e2. [PubMed: 19663808]

Fawaz CS, Martel P, Leo D, Trudeau LE. Presynaptic action of neurotensin on dopamine release through inhibition of D(2) receptor function. BMC Neurosci 2009;10:96. [PubMed: 19682375]

Fowler SC, Birkestrand BR, Chen R, Moss SJ, Vorontsova E, Wang G, Zarcone TJ. A force-plate actometer for quantitating rodent behaviors: illustrative data on locomotion, rotation, spatial patterning, stereotypies, and tremor. J Neurosci Methods 2001;107:107–124. [PubMed: 11389948]

Geter-Douglass B, Katz JL, Alling K, Acri JB, Witkin JM. Characterization of unconditioned behavioral effects of dopamine D3/D2 receptor agonists. J Pharmacol Exp Ther 1997;283:7–15. [PubMed: 9336302]

Hardin SC, Larue CT, Oh MH, Jain V, Huber SC. Coupling oxidative signals to protein phosphorylation via methionine oxidation in Arabidopsis. Biochem J 2009;422:305–312. [PubMed: 19527223]

Harrison C, Traynor JR. The [35S]GTPgammaS binding assay: approaches and applications in pharmacology. Life Sci 2003;74:489–508. [PubMed: 14609727]

Hickey MA, Reynolds GP, Morton AJ. The role of dopamine in motor symptoms in the R6/2 transgenic mouse model of Huntington's disease. J Neurochem 2002;81:46–59. [PubMed: 12067237]

Hornykiewicz O. Dopamine (3-hydroxytyramine) in the central nervous system and its relation to the Parkinson syndrome in man. Dtsch Med Wochenschr 1962;87:1807–1810. [PubMed: 14448985]

Ilani T, Fishburn CS, Levavi-Sivan B, Carmon S, Raveh L, Fuchs S. Coupling of dopamine receptors to G proteins: studies with chimeric D2/D3 dopamine receptors. Cell Mol Neurobiol 2002;22:47–56. [PubMed: 12064517]

Johnson MA, Rajan V, Miller CE, Wightman RM. Dopamine release is severely compromised in the R6/2 mouse model of Huntington's disease. J Neurochem 2006;97:737–746. [PubMed: 16573654]

Koeltzow TE, Austin JD, Vezina P. Behavioral sensitization to quinpirole is not associated with increased nucleus accumbens dopamine overflow. Neuropharmacology 2003;44:102–110. [PubMed: 12559127]

Kraft JC, Osterhaus GL, Ortiz AN, Garris PA, Johnson MA. In vivo dopamine release and uptake impairments in rats treated with 3-nitropropionic acid. Neuroscience 2009;161:940–949. [PubMed: 19362126]

Lan H, Liu Y, Bell MI, Gurevich VV, Neve KA. A dopamine D2 receptor mutant capable of G protein-mediated signaling but deficient in arrestin binding. Mol Pharmacol 2009;75:113–123. [PubMed: 18809670]

Levant B, Grigoriadis DE, DeSouza EB. Characterization of [3H]quinpirole binding to D2-like dopamine receptors in rat brain. J Pharmacol Exp Ther 1992;262:929–935. [PubMed: 1356154]

Lieberman JA, Bymaster FP, Meltzer HY, et al. Antipsychotic drugs: comparison in animal models of efficacy, neurotransmitter regulation, and neuroprotection. Pharmacol Rev 2008;60:358–403. [PubMed: 18922967]

Montmayeur JP, Guiramand J, Borrelli E. Preferential coupling between dopamine D2 receptors and G-proteins. Mol Endocrinol 1993;7:161–170. [PubMed: 7682286]

Moskovitz J. Methionine sulfoxide reductases: ubiquitous enzymes involved in antioxidant defense, protein regulation, and prevention of aging-associated diseases. Biochim Biophys Acta 2005;1703:213–219. [PubMed: 15680229]

Moskovitz J, Rahman MA, Strassman J, Yancey SO, Kushner SR, Brot N, Weissbach H. Escherichia coli peptide methionine sulfoxide reductase gene: regulation of expression and role in protecting against oxidative damage. J Bacteriol 1995;177:502–507. [PubMed: 7836279]

Moskovitz J, Berlett BS, Poston JM, Stadtman ER. The yeast peptide-methionine sulfoxide reductase functions as an antioxidant in vivo. Proc Natl Acad Sci USA 1997;94:9585–9589. [PubMed: 9275166]

Moskovitz J, Flescher E, Berlett BS, Azare J, Poston JM, Stadtman ER. Overexpression of peptide-methionine sulfoxide reductase in Saccharomyces cerevisiae and human T cells provides them with high resistance to oxidative stress. Proc Natl Acad Sci USA 1998;95:14071–14075. [PubMed: 9826655]

Moskovitz J, Bar-Noy S, Williams WM, Requena J, Berlett BS, Stadtman ER. Methionine sulfoxide reductase (MsrA) is a regulator of antioxidant defense and lifespan in mammals. Proc Natl Acad Sci USA 2001;98:12920–12925. [PubMed: 11606777]

Namkung Y, Dipace C, Javitch JA, Sibley DR. G protein-coupled receptor kinase-mediated phosphorylation regulates post-endocytic trafficking of the D2 dopamine receptor. J Biol Chem 2009;284:15038–15051. [PubMed: 19332542]

Niimi K, Takahashi E, Itakura C. Age dependence of motor activity and sensitivity to dopamine receptor 1 agonist, SKF82958, of inbred AKR/J, BALB/c, C57BL/6J, SAMR1, and SAMP6 strains. Brain Res 2009;1250:175–182. [PubMed: 19007759]

Nwaneshiudu CA, Unterwald EM. Blockade of neurokinin-3 receptors modulates dopamine-mediated behavioral hyper-activity. Neuropharmacology 2009;57:295–301. [PubMed: 19500601]

Oien DB, Moskovitz J. Substrates of the methionine sulfoxide reductase system and their physiological relevance. Curr Top Dev Biol 2008;80:93–133. [PubMed: 17950373]

Oien DB, Osterhaus GL, Latif SA, Pinkston JW, Fulks J, Johnson M, Fowler SC, Moskovitz J. MsrA knockout mouse exhibits abnormal behavior and brain dopamine levels. Free Radic Biol Med 2008;45:193–200. [PubMed: 18466776]

Oien DB, Shinogle HE, Moore DS, Moskovitz J. Clearance and phosphorylation of alpha-synuclein are inhibited in methionine sulfoxide reductase a null yeast cells. J Mol Neurosci 2009;39:323–332. [PubMed: 19653131]

Pahwa R, Lyons KE, Hauser RA. Ropinirole therapy for Parkinson's disease. Expert Rev Neurother 2004;4:581–588. [PubMed: 15853577]

Pal R, Oien DB, Ersen FY, Moskovitz J. Elevated levels of brain-pathologies associated with neurodegenerative diseases in the methionine sulfoxide reductase A knockout mouse. Exp Brain Res 2007;180:765–774. [PubMed: 17333008]

Romero HM, Berlett BS, Jensen PJ, Pell EJ, Tien M. Investigations into the role of the plastidial peptide methionine sulfoxide reductase in response to oxidative stress in Arabidopsis. Plant Physiol 2004;136:3784–3794. [PubMed: 15516509]

Ruan H, Tang XD, Chen ML, et al. High-quality life extension by the enzyme peptide methionine sulfoxide reductase. Proc Natl Acad Sci USA 2002;99:2748–2753. [PubMed: 11867705]

Saxena S, Brody AL, Schwartz JM, Baxter LR. Neuroimaging and frontal-subcortical circuitry in obsessive-compulsive disorder. Br J Psychiatry Suppl 1998;35:26–37. [PubMed: 9829024]

Usiello A, Baik JH, Rouge-Pont F, Picetti R, Dierich A, LeMeur M, Piazza PV, Borrelli E. Distinct functions of the two isoforms of dopamine D2 receptors. Nature 2000;408:199–203. [PubMed: 11089973]

Walss-Bass C, Soto-Bernardini MC, Johnson-Pais T, et al. Methionine sulfoxide reductase: a novel schizophrenia candidate gene. Am J Med Genet B Neuropsychiatr Genet 2009;150B:219–225. [PubMed: 18506707]

Wang Y, Xu R, Sasaoka T, Tonegawa S, Kung MP, Sankoorikal EB. Dopamine D2 long receptor-deficient mice display alterations in striatum-dependent functions. J Neurosci 2000;20:8305–8314. [PubMed: 11069937]

Zhang Y, D'Souza D, Raap DK, Garcia F, Battaglia G, Muma NA, Van de Kar LD. Characterization of the functional heterologous desensitization of hypothalamic 5-HT(1A) receptors after 5-HT(2A) receptor activation. J Neurosci 2001;21:7919–7927. [PubMed: 11588165]

Zhang L, Yu C, Vasquez FE, Galeva N, Onyango I, Swerdlow RH, Dobrowsky RT. Hyperglycemia alters the schwann cell mitochondrial proteome and decreases coupled respiration in the absence of superoxide production. J Proteome Res 2010;9:458–471. [PubMed: 19905032]

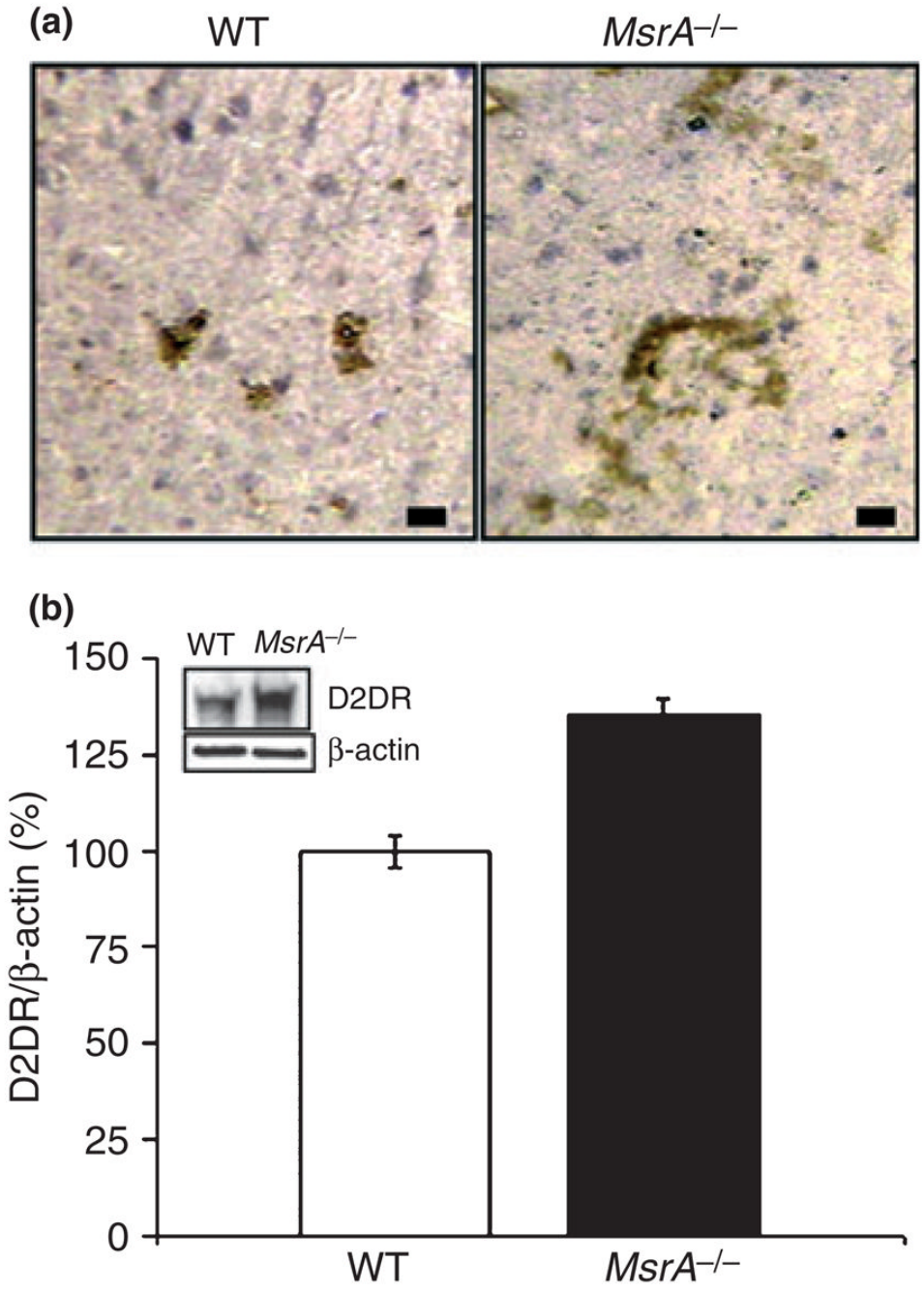

Fig. 1.

Immunohistochemistry and immunoblot analyses of D2DR in *MsrA*−/− and WT striatum. (a) Immunohistochemistry of coronal brain sections using primary antibodies against D2DR. Slides were visualized using light microscope with a 100× objective lens. Brownish structures correspond to the presence of D2DR. Scale bars represent 10 μm. (b) Immunoblot analysis using primary antibodies against D2DR. Representative bands are shown in the small window followed by densitometry analysis for the corresponding D2DR band in each extract (relative density in WT represents 100%; $p < 0.01$, *t*-test). The densities of D2DR were corrected for the relative densities of β-actin.

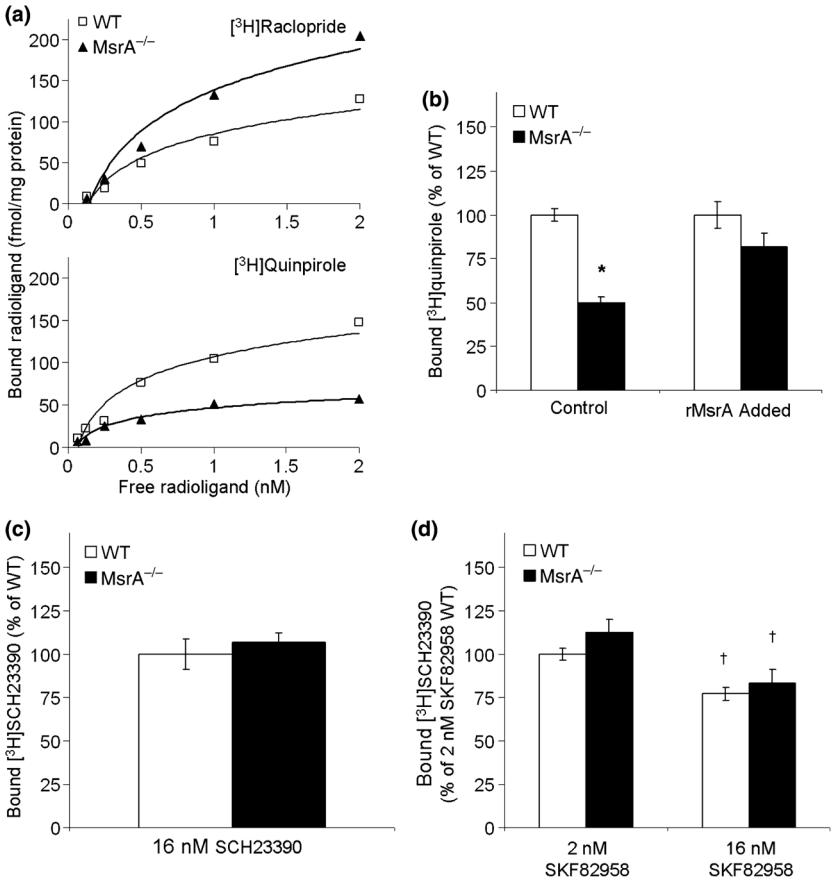

Fig. 2.

Binding efficiency of ligands to D2DR and D1DR in *MsrA*−/− and WT membranes. Specific ligand binding was calculated from subtracting non-specific ligand binding from total ligand binding as described in 'Materials and Methods'. (a) Representative [^{3}H]raclopride and [^{3}H] quinpirole specific ligand binding curves of D2DR. (b) B_{max} of [^{3}H]quinpirole binding presented as percent of WT B_{max} value (represents 100% binding) in the absence (Control) and presence of recombinant yeast MsrA (rMsrA Added). (c) Binding of [^{3}H]SCH23390 at a saturating concentration (B_{max} value WT, under these conditions, represents 100% binding). (d) Relative binding of [^{3}H]SCH23390 at a concentration of 2 nM (as in panel c) in the presence of 2 nM and 16 nM SKF82958 concentrations. For all graphs, $n = 3$. Significance is denoted by * or † indicating $p < 0.05$ using *t*-test for difference by mouse type or by condition, respectively.

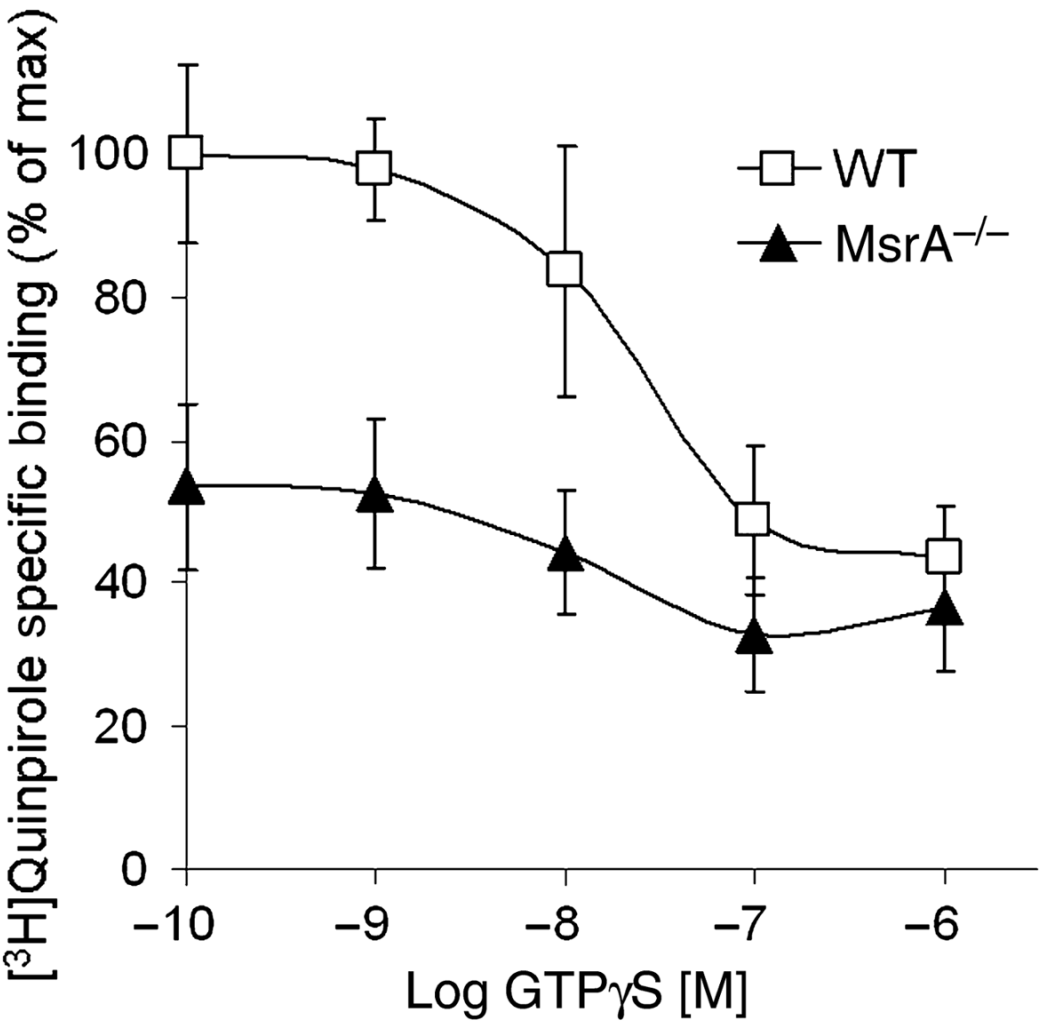

Fig. 3.

Inhibition of D2DR agonist binding in striatal membrane extracts of *MsrA*−/− and WT mice in the presence of GTPγS. The Y axis values of the graph represent the specific binding percentage of [^{3}H]quinpirole at GTPγS concentrations of 0.1, 1, 10, 100, and 1000 nM. The value at 100% specific binding represents maximum binding of WT D2DR to [^{3}H]quinpirole at 0.1 nM GTPγS. The maximum binding values were not significantly different from values obtained in the absence of GTPγS; data not shown, $n = 3$.

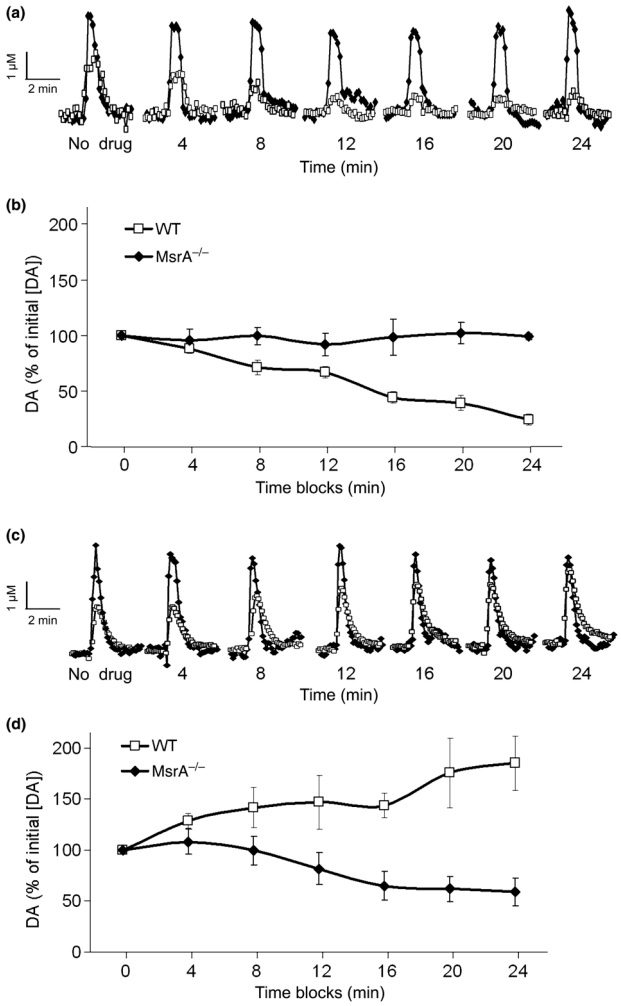

Fig. 4.

DA release in striatal sections from *MsrA*−/− and WT mice treated with D2DR agonist and antagonist. Coronal sections were stimulated using a 30 pulse-stimulus train and DA scans were collected by fast scan cyclic voltammetry. (a) A representative stimulated DA release plot generated from measurements in the presence and absence of quinpirole. WT, *open squares; MsrA*−/−, *filled diamonds*. (b) The DA release measured in 4-min time blocks of WT and *MsrA*−/− sections in the presence of quinpirole. The basal initial measurements without drug treatment (time block 0) were set to 100%. All subsequent measurements with quinpirole are represented as a percentage of this value. (c) A representative stimulated DA release plot generated from measurements obtained in the presence and absence of sulpiride. WT, *open squares; MsrA*−/−, *filled diamonds*. (d) The DA release measured in 4-min time blocks of WT and *MsrA*−/− sections in the presence of sulpiride. The initial basal measurements without treatment (time block 0) were set to 100%. All subsequent measurements with sulpiride are represented as a percentage of the initial 100% values. For both experiments, $n = 3$ and $p < 0.05$ for genotype determined by two-way repeated measures ANOVA. The basal DA concentrations in the absence of drug were WT = 1.63 ± 0.44 μM and *MsrA*−/− = 5.47 ± 0.36 μM.

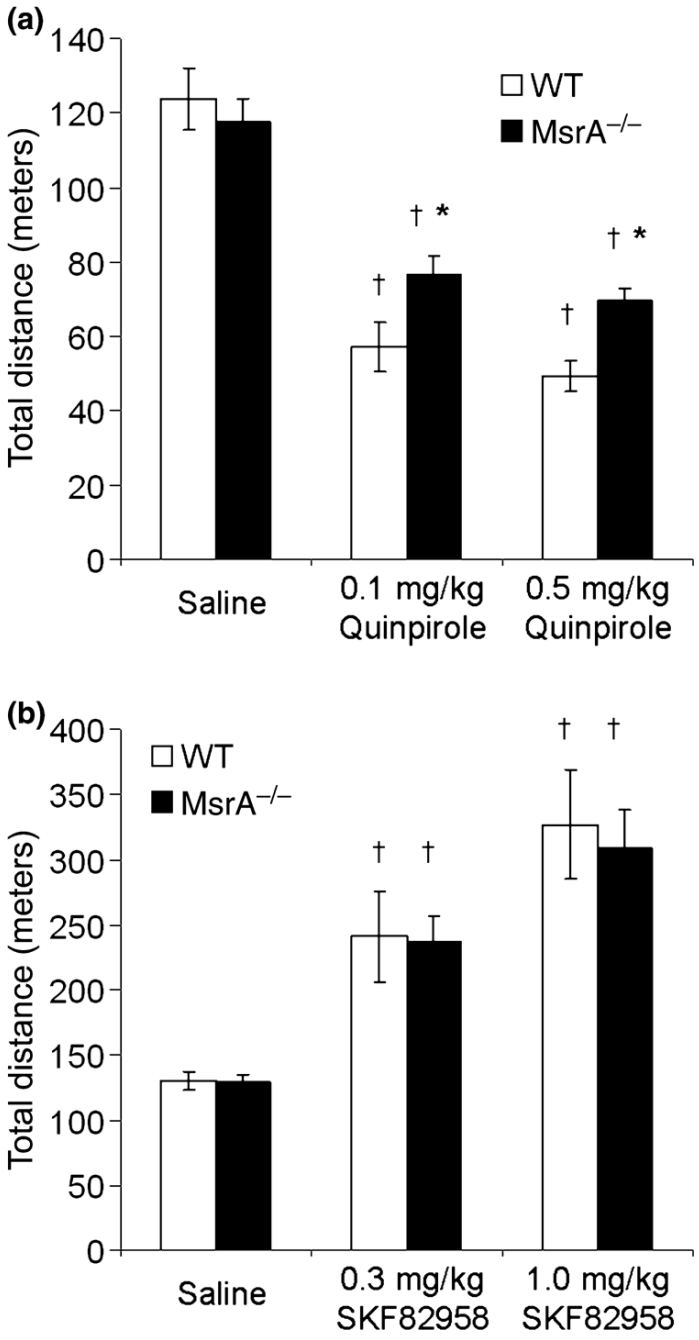

Fig. 5.

Locomotor activity after D2DR and D1DR agonist administration in *MsrA*−/− and WT mice. Total distance traveled was measured for 45 min after intraperitoneal injections of saline (vehicle) or indicated drug. (a) Quinpirole injection at doses of 0.5 mg/kg and 0.1 mg/kg. WT, $n = 7$; *MsrA*−/−, $n = 10$. $^{\dagger}p < 0.01$ for quinpirole effect and $*p < 0.02$ for the genotype effect, determined by ANOVA. (b) SKF82958 injection at doses of 0.3 mg/kg and 1.0 mg/kg. WT, $n = 7$; *MsrA*−/−, $n = 10$. There was no significant effect of mouse type on SKF82958 effect, SKF82958 increased locomotor activity in the dose range used ($^{\dagger}p < 0.01$) and no dose-by-type interaction was detected; determined by ANOVA.

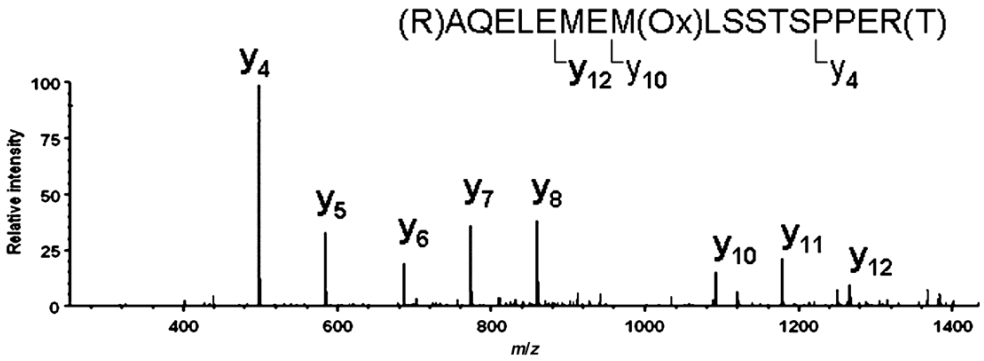

D2DR third intracellular loop sequence (amino acids: 211-375):

211kiyivlrkrrkrvntkrssrafranlktplkgncthpedmklctvimksngsfpvnrrrmdaarr(aqelememlsstsppe r)tryspippshhqltlpdpshhglhsnpdspakpeknghakivnpriakffeiqtmpngktrtslktmsrrklsqqkekkatq m375

Percent Met (Y10) oxidation (-blank)

+H_2O_2: 2.00 ± 0.10

+H_2O_2 + rMsrA: 0.80 ± 0.05

Fig. 6.

Oxidized methionine residues in $D2DR_L$-IC_3 recombinant protein. The short and long form D2DR differ by a 29-amino-acid region in the third cytoplasmic loop, which begins after amino acid 241 in the rat sequence (underlined). The methionines (m) are in bold. The corresponding recombinant fusion protein GST-$D2DR_L$-IC_3 was isolated and resulting peptides were subjected to tandem mass spectrometry after trypsin digestion. The sequence of the major oxidized peptide identified is shown and also indicated in the sequence by parenthesis. Representative relative signal levels for the daughter ions of the major peptide detected after collision-induced fragmentation are presented as relative intensity of each ion. The difference in percent methionine (Y10) oxidation between the presence and absence of rMsrA was found to be significant (three experiments, $p < 0.05$ by *t*-test).